International Journal of Fatigue 30 (2008) 2175–2190

Contents lists available at ScienceDirect

International Journal of Fatigue

journal homepage: www.elsevier.com/locate/ijfatigue

# Fatigue behavior of aluminum 5754-O and 6111-T4 spot friction welds in lap-shear specimens

V.-X. Tran [a], J. Pan [a,*], T. Pan [b]

[a] Mechanical Engineering, University of Michigan, Ann Arbor, MI 48109, USA
[b] Ford Research and Advanced Engineering, Ford Motor Company, Dearborn, MI 48131, USA

ARTICLE INFO

*Article history:*
Received 2 December 2007
Received in revised form 20 May 2008
Accepted 23 May 2008
Available online 13 June 2008

*Keywords:*
Spot friction weld
Friction stir spot weld
Failure mode
Fatigue life
Kinked crack
Structural stress

ABSTRACT

Fatigue behavior of aluminum 5754-O and 6111-T4 spot friction welds in lap-shear specimens is investigated based on experimental observations and two fatigue life estimation models. Optical micrographs of the 5754 and 6111 welds made by a concave tool and a flat tool, respectively, before and after failure under quasi-static and cyclic loading conditions are examined. The micrographs show that the failure modes of the 5754 and 6111 welds under quasi-static and cyclic loading conditions are quite different. Under quasi-static loading conditions, both types of welds mainly fail from the nearly flat fracture surface through the nugget. Under low-cycle loading conditions, both types of welds mainly fail from the kinked crack through the upper sheet thickness and the fracture surface through the nugget. Under high-cycle loading conditions, both types of welds mainly fail from the kinked cracks through the upper and lower sheet thicknesses. A kinked fatigue crack growth model based on the stress intensity factor solutions for finite kinked cracks and a structural stress model based on the closed-form structural stress solutions at the critical locations of the welds are adopted to estimate the fatigue lives of both types of welds. The fatigue life estimations based on the kinked fatigue crack growth model and the structural stress model appear to agree well with the experimental results for both types of welds.



## 1. Introduction

Resistance spot welding is the most commonly used joining technique for body-in-white parts made of steel sheets. However, resistance spot welding of aluminum sheets is likely to produce poor welds as reported by Thornton et al. [1] and Gean et al. [2]. Recently, a spot friction welding technology for joining aluminum sheets has been developed by Mazda Motor Corporation and Kawasaki Heavy Industry [3,4]. The most significant advantage of the spot friction welding process comparing to the conventional welding processes is that the joint can be made without melting the base metal. A schematic illustration of the spot friction welding process was presented, for example, in Lin et al. [5].

The mechanical behavior of aluminum spot friction welds under quasi-static loading conditions was studied, for example, see Lin et al. [5], Pan et al. [6], Fujimoto et al. [7,8] and Hinrichs et al. [9]. The metallurgical aspects of aluminum 6111 spot friction welds were investigated by Mitlin et al. [10]. Tran et al. [11] investigated the failure loads of spot friction welds in aluminum 6111 lap-shear specimens under quasi-static and dynamic loading conditions. Recently, Lin et al. [12–15] investigated the fatigue behavior of spot friction welds made by different tools in aluminum 6111 sheets based on experimental observations and fracture mechanics. A comprehensive literature review for spot friction welds can be found in Pan [16]. Note that most of the literature is for spot friction welds between similar aluminum sheets. However, dissimilar spot friction welds between aluminum 2017-T6 and 5052 sheets, between aluminum 5754 and 6111 sheets, and between aluminum 5754-O and 7075-T6 sheets were investigated by Tozaki et al. [17], Su et al. [18] and Tran et al. [19], respectively.

It should be noted that aluminum 5754 alloys are widely employed in the automotive industry to produce parts such as internal door stiffeners or the entire body-in-white as reported in Kaufman [20]. However, the fatigue behavior of aluminum 5754 spot friction welds has not been extensively studied. In this paper, we investigate the fatigue behavior of aluminum 5754 and 6111 spot friction welds in lap-shear specimens based on experimental observations and two fatigue life estimation models. Optical micrographs of the welds before and after failure under quasi-static and cyclic loading conditions are examined to investigate the fracture and failure mechanisms of both types of welds. Based on the experimental observations of the paths of the dominant kinked fatigue cracks, the kinked fatigue crack growth model as discussed in Lin et al. [12–15] with the global stress intensity factor solutions for the main cracks obtained from three-dimensional finite element analyses is adopted to estimate the fatigue lives of the welds. The structural stress model based on the closed-form structural

* Corresponding author. Tel.: +1 734 764 9404; fax: +1 734 647 3180.
*E-mail address:* jwo@umich.edu (J. Pan).

0142-1123/$ - see front matter © 2008 Elsevier Ltd. All rights reserved.
doi:10.1016/j.ijfatigue.2008.05.025

stress solutions at the critical locations of the spot welds as reported in Lin and Pan [21] and the experimental stress-life fatigue data is also adopted to estimate the fatigue lives of the welds. Finally, the estimated fatigue lives based on the kinked fatigue crack growth model and the structural stress model are compared with the experimental results for both types of welds.

## 2. 5754 and 6111 spot friction welds before testing

For the spot friction welding process under load-controlled conditions, the important welding processing parameters are the tool geometry, the tool rotational speed, the tool downward force and the processing time. In this investigation, a tool with a concave shoulder and a threaded probe pin was used to make spot friction welds in lap-shear specimens of aluminum 5754-O sheets of the thickness of 2.0 mm. A tool rotational speed of 3000 rpm and a tool downward force of 5.88 kN were specified to make the 5754 spot friction welds. The 5754 welds were first made at different processing times and tested under lap-shear loading conditions. The optimal processing time for the maximum failure strength of the 5754 welds in lap-shear specimens under this particular set of the welding processing parameters was identified. This optimal processing time and the welding processing parameters specified above were then used to make the 5754 spot friction welds tested in this investigation.

In this investigation, another tool with a flat shoulder was used to make spot friction welds in lap-shear specimens of aluminum 6111-T4 sheets. For the 6111 welds, the thicknesses of the upper and lower sheets are 0.94 mm and 1.04 mm, respectively. The 6111 welds tested in this investigation were made based on a DOE (design of experiments) method to determine the optimal tool rotational speed, tool downward force and processing time for the maximum failure strength of the 6111 welds in lap-shear specimens. Note that the 6111 lap-shear specimens used in this investigation and those used in Tran et al. [11] are identical. The 6111 lap-shear specimens used in this investigation were made of the upper and lower sheets of unequal thicknesses while the 6111 lap-shear specimens used in Lin et al. [13,15] were made of the upper and lower sheets of equal thickness. We first present some optical and scanning electron micrographs of the cross sections along the symmetry planes of the 5754 and 6111 spot friction welds before testing.

Fig. 1a shows an optical micrograph of the cross section along the symmetry plane of a 5754 spot friction weld made by the concave tool before testing. As shown in the figure, the indentation profile reflects the general shape of the threaded probe pin and the concave shoulder of the tool. The bottom surface of the lower sheet is almost flat. The area near the central hole represents the fine grain stir zone where the upper and lower sheets are well bonded possibly due to high pressure and large plastic deformation. Two notches, marked as N1 and N2, can be seen in the figure. Fig. 1b shows a close-up optical micrograph of region I in Fig. 1a, where the notch, marked as N2, extends and becomes a crack. The location of the crack tip is marked in the figure. Fig. 1c shows a close-up optical micrograph of region II in Fig. 1b. As shown in Fig. 1c, the interfacial surface between the two deformed sheet materials materials near the crack tip slightly rises up outside the stir zone. The location of the crack tip is also marked in the figure. The location of the crack tip can be identified by a scanning electron micrograph of the crack tip region as shown in Fig. 1d. As shown in the figure, some part of the crack surface near the tip becomes vague and may be bonded by the welding process.

As shown in Fig. 1a, the thickness of the weld nugget near the central hole is slightly larger than that near the outer circumference of the tool shoulder indentation due to the concave geometry of the tool shoulder. The concave tool shoulder squeezed out some upper sheet material but maintained some upper sheet material near the central hole. As suggested in Fig. 1a, the material under the tool shoulder indentation flowed outward and resulted in a radial expansion of the upper sheet material along the outer circumference of the tool shoulder indentation. However, due to the constraint of the neighboring material, the upper sheet was therefore slightly bent along the outer circumference of the tool shoulder indentation.

Fig. 2a shows an optical micrograph of the cross section along the symmetry plane of a 6111 spot friction weld made by the flat tool before testing. As shown in the figure, the indentation profile reflects the shape of the probe pin and the flat shoulder of the tool. The bottom surface of the lower sheet is almost flat. The area near the central hole represents the fine grain stir zone where the upper and lower sheets are well bonded possibly due to high pressure and large plastic deformation. Two notches, marked as N1 and N2, can be seen in the figure. Fig. 2b shows a close-up optical micrograph of region I in Fig. 2a, where the notch, marked as N2, extends and becomes a crack. The location of the crack tip is marked in the figure. Fig. 2c shows a close-up optical micrograph of region II in Fig. 2b where the interfacial surface, marked by two small arrows, becomes vague and disappears into the stir zone. As shown in Fig. 2c, the interfacial surface between the two deformed sheet materials near the crack tip remained almost planar outside the stir zone. The location of the crack tip is also marked in the figure. The location of the crack tip can also be identified by a scanning electron micrograph of the crack tip region as shown in Fig. 2d. As shown in the figure, some part of the crack surface near the tip becomes vague and may be bonded by the welding process.

As shown in Fig. 2a, the flat tool shoulder squeezed out a portion of the upper sheet material and, consequently, the thickness of the upper sheet decreased under the shoulder indentation. As suggested in Fig. 2a, the material under the tool shoulder indentation flowed outward and resulted in a radial expansion of the upper sheet material along the outer circumference of the shoulder indentation. However, due to the constraint of the neighboring material, the upper sheet was therefore slightly bent along the outer circumference of the tool shoulder indentation.

## 3. Experiments

The lap-shear specimens were made by using two 25.4 mm by 101.6 mm aluminum sheets with a 25.4 mm by 25.4 mm overlap area. Figs. 3a and b show a 5754 lap-shear specimen with a spot friction weld made by the concave tool and a 6111 lap-shear specimen with a spot friction weld made by the flat tool, respectively. As shown in Fig. 3a, two square doublers of 25.4 mm $\times$ 25.4 mm made of aluminum 5754 sheets are attached to the ends of the 5754 lap-shear specimen. As shown in Fig. 3b, two doublers are made by folding two square parts of the sheets near the ends (25.4 mm $\times$ 25.4 mm) of the 6111 lap-shear specimen. Note that the doublers are used to align the applied load to avoid the initial realignment of the specimen under lap-shear loading conditions and to reinforce the sheet materials near the holes. Due to the load-controlled welding process, the actual plunge depths of the tool penetration and the geometries of the spot friction welds may not be controlled precisely under the same welding processing parameters. In order to minimize the effects of the weld geometry on the experimental results, we selected the specimens with the spot friction welds that have nearly the same actual plunge depths of the tool penetration for the quasi-static and fatigue tests. Before testing, all 6111 specimens were baked in an oven at 170 °C for 20 minutes and cooled in the ambient air to simulate the paint bake cycles in automotive assembly plants.

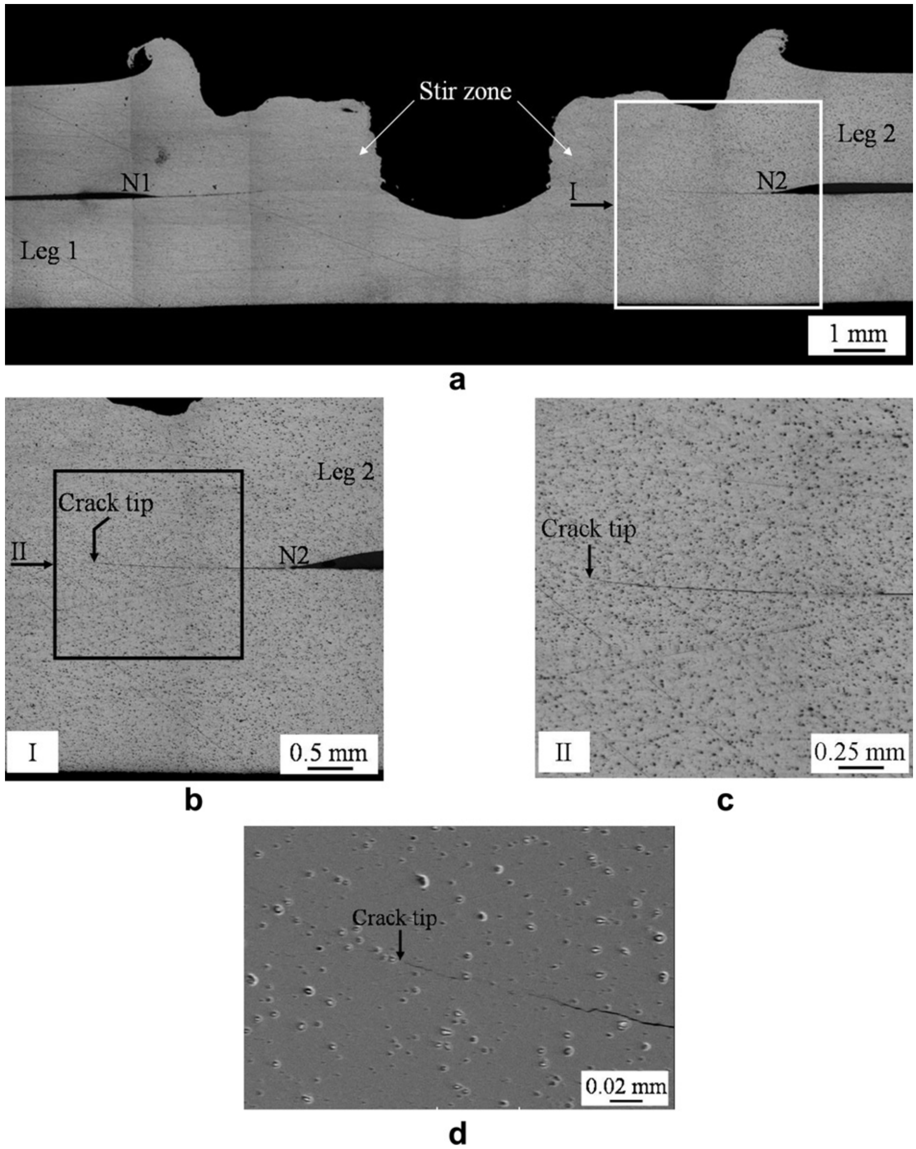


**Fig. 1.** (a) An optical micrograph of the cross section along the symmetry plane of a 5754 spot friction weld made by the concave tool before testing, (b) a close-up optical micrograph of region I, (c) a close-up optical micrograph of region II, (d) a close-up scanning electron micrograph of the crack tip region as shown in (c).

Lap-shear specimens were first tested under quasi-static loading conditions by using an Instron testing machine at a monotonic displacement rate of 1.0 mm per minute. The load and displacement were simultaneously recorded during each test. The average failure loads, defined as the maximum loads of the load–displacement curves, obtained from three tested 5754 and 6111 lap-shear specimens are 4.34 kN and 3.38 kN, respectively. These failure loads were used as the reference loads to determine the loads applied in the fatigue tests. The lap-shear specimens were then tested under cyclic loading conditions by using an Instron servo-hydraulic fatigue testing machine with the load ratio $R$ of 0.2. The test frequency was 10 Hz. The tests were terminated when specimens were separated, or nearly separated when the displacement of the two grips of specimens exceeded 5 mm. Some tests were stopped before the final failures of the specimens to examine the fatigue crack growth patterns. Fig. 3c shows the experimental results for the 5754 spot friction welds made by the concave tool and the 6111 spot friction welds made by the flat tool in lap-shear specimens under cyclic loading conditions. The number of specimens available for fatigue testing is limited.

## 4. Failure modes of 5754 welds under quasi-static and cyclic loading conditions

### 4.1. A two-dimensional overview of failure modes

We conducted experiments for the 5754 spot friction welds in lap-shear specimens under quasi-static and cyclic loading conditions. Based on the experimental observations, the failed 5754 spot friction welds under quasi-static loading conditions show one failure mode. The failed 5754 spot friction welds under cyclic loading conditions with the fatigue lives from $10^3$ cycles to $10^4$ cycles (low-cycle fatigue) show a different failure mode. The failed 5754 spot friction welds under cyclic loading conditions with the fatigue lives from $10^4$ cycles to $2 \times 10^5$ cycles (high-cycle fatigue) show another failure mode. Note that we define low-cycle fatigue and high-cycle fatigue loading conditions only for convenient presentation in this paper. The fatigue life and the load range for the transition of the failure mode from low-cycle fatigue to high-cycle fatigue for the 5754 spot friction welds are about $1.46 \times 10^4$ cycles and 2.01 kN, respectively, as shown in Fig. 3c. Since the failure modes of the